

Hammer events, neutrino energies, and nucleon-nucleon correlations

L.B. Weinstein,^{1,*} O. Hen,² and Eli Piasetzky³

¹ *Old Dominion University, Norfolk, VA 23529, USA*

² *Massachusetts Institute of Technology, Cambridge, MA 02139, USA*

³ *Tel Aviv University, Tel Aviv 69978, Israel*

(Dated: June 16, 2022)

Background: Accelerator-based neutrino oscillation measurements depend on observing a difference between the expected and measured rate of neutrino-nucleus interactions at different neutrino energies or different distances from the neutrino source. Neutrino-nucleus scattering cross sections are complicated and depend on the neutrino beam energy, the neutrino-nucleus interaction, and the structure of the nucleus. Knowledge of the incident neutrino energy spectrum and neutrino-detector interactions are crucial for analyzing neutrino oscillation experiments. Short range nucleon-nucleon correlations in nuclei (NN SRC) affect properties of nuclei. The ArgoNeut liquid Argon Time Projection Chamber (lArTPC) observed charged-current neutrino-argon scattering events with two protons back-to-back in the final state (“hammer” events) which they associated with SRC pairs. The large volume MicroBoone lArTPC will measure far more of these unique events.

Purpose: Determine what we can learn about the incident neutrino energy spectrum and/or the structure of SRC from hammer events that will be measured in MicroBooNE.

Methods: We simulate hammer events using two simple models. We take advantage of the well known electron-nucleon scattering cross section to calculate electron-argon interactions in a simple model where the electron scatters from a moving proton, ejecting a π^+ , and the π^+ is then absorbed on a moving deuteron-like np pair. We also calculate interactions in a second model where the electron scatters from a moving nucleon, exciting it to a Δ or N^* , which then deexcites by interacting with a second nucleon: $\Delta N \rightarrow pp$. These simple models do not include the effects of rescattering of the two final-state protons as they exit the residual nucleus.

Results: The pion production and reabsorption process results in two back-to-back protons each with momentum of about 500 MeV/c, very similar to that of the observed ArgoNeut events. These distributions are insensitive to either the relative or center-of-mass momentum of the np pair that absorbed the π . In this model, the incident neutrino energy can be reconstructed relatively accurately using the outgoing lepton. The $\Delta p \rightarrow pp$ process results in two protons that are less similar to the observed events.

Conclusions: ArgoNeut hammer events can be described by a simple pion production and reabsorption model. These hammer events in MicroBooNE can be used to determine the incident neutrino energy but not to learn about SRC.

Since the incident neutrino energy of these hammer events can be accurately reconstructed (at typical MicroBooNE neutrino energies) from just the scattered lepton, we suggest that this reaction channel could be used for neutrino oscillation experiments to complement other channels with higher statistics but different systematic uncertainties.

PACS numbers: 13.15.+g, 25.30.Pt, 25.10.+s

Introduction: Neutrino scattering from nuclei can be used to learn about both the energy distribution of the incident neutrino beam and the neutrino-nucleus interaction. The neutrino beam energy distribution is necessary to interpret the results of neutrino oscillation experiments [1]. The neutrino-nucleus interaction can be used to understand the neutrino-detector interactions which complicate interpretation of neutrino experiments or to learn more about the structure of nuclei.

With large-volume liquid-argon time projection chambers (lArTPCs), neutrino scattering experiments can measure all of the charged particles emitted in an interaction, helping disentangle the effects of the neutrino energy distribution, the neutrino-nucleus interaction, and nuclear structure.

An important class of nuclear structure effects is due to Short Range Correlated two-nucleon pairs (NN SRC).

SRC pairs account for about 20% of nucleons, almost all of the high momentum ($k > k_F \approx 250$ MeV/c) nucleons, and most of the kinetic energy in medium to heavy nuclei [2–8]. They are composed predominantly of neutron-proton np correlated pairs, even in heavy, neutron-rich, asymmetric nuclei [7, 9].

Since the incident neutrino energy for each event is inferred from the detected final state particles, it is important to include the effects of two nucleon currents and SRC pairs when analyzing neutrino-nucleus reactions [10, 11].

Our knowledge of the composition and distribution of SRC comes predominantly from high energy electron scattering, where the electron scatters from a high-momentum ($k > k_F$) proton. In one type of experiment, the scattered electron and the knocked out proton are detected and a large acceptance detector is placed to look

for the correlated partners, if any, of the knocked-out proton, $A(e, e'p)$ and $A(e, e'pN)$ [7–9]. In this experiment, the two nucleons in the SRC are back-to-back in the initial nucleus. Another type of experiment involved measuring the ${}^3\text{He}(e, e'pp)n$ reaction by scattering electrons from ${}^3\text{He}$ and detecting the scattered electrons and the emitted protons in a 4π spectrometer [12, 13]. That experiment detected many events where the electron scattered from a single nucleon, and the residual spectator pair emerged back-to-back in the lab frame (in the final state).

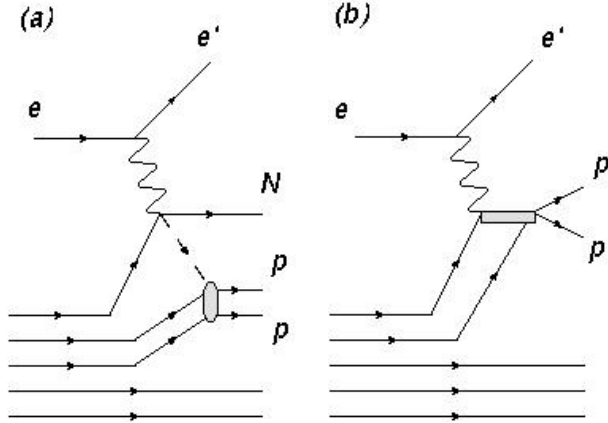


FIG. 1: Pictorial diagram of neutrino induced two-proton knockout $\text{Ar}(\nu, \mu^- pp)$. (a) The neutrino scatters from a first nucleon, emitting a pion. The pion is absorbed by two nucleons, which are detected. (b) The neutrino scatters from a first nucleon, exciting it to a resonance, which deexcites via $\Delta N \rightarrow pp$.

The ArgoNeut large-volume liquid-argon time projection chamber (TPC) in the Main Injector neutrino beam at Fermilab has detected 19 events with two high-momentum ($k > k_F$) protons and no pions in the final state, $\text{Ar}(\nu, \mu^- pp)$ [14]. Of these, four events have reconstructed nucleons back-to-back in the initial nucleus and four more have two protons back-to-back in the lab frame (hammer events).

The first set of events corresponds to the $A(e, e'pN)$ measurements described above where the projectile scatters from one nucleon in the correlated pair and its correlated partner then emerges from the nucleus.

The second set of events is attributed to resonance production on the struck nucleon, followed by pion emission and absorption on the correlated pair (see Fig. 1a). The authors claim that, “The detection of back-to-back pp pairs in the lab frame can be seen as snapshots of the initial pair configuration in the case of RES processes with no or low momentum transfer to the pair.”

The much larger MicroBooNE liquid-argon TPC should detect far more of these intriguing events.

In this paper we will develop two simple semi-classical models of these hammer events. The first model will

describe pion production on a nucleon followed by pion absorption on an NN pair (see Fig. 1a) and the second model will describe resonance excitation (primarily $\Delta(1232)$) followed by deexcitation via the reaction $\Delta N \rightarrow pp$ (see Fig. 1b). We will show that, contrary to the claims of Ref. [14], the final state distribution of pp pairs in the first model is relatively insensitive to the details of the “initial pair configuration”. However, we will also show that the incident neutrino energy can be reconstructed from the momentum of the outgoing muon with or without the momenta of the two outgoing protons.

Methods: We describe the reaction process of Fig. 1a by a sequential pion production and absorption model. We use the MAID-2000 [15] parametrization to take advantage of the well measured pion-electroproduction cross section. While the electron ($e, e'\pi$) and charged-current neutrino ($\nu, \mu^-\pi$) pion production cross sections differ in detail, both are $\Delta(1232)$ -dominated in this energy region and both are transverse. Therefore both processes should produce similar pion momentum distributions.

We generate a nucleon with initial momentum according to the ${}^{12}\text{C}$ Argonne V18 momentum distribution [16], randomly sample the initial electron energy from the MiniBooNE neutrino energy distribution [17], and uniformly generate the scattered electron energy and angles and the emitted pion angles. We then calculate the cross section using MAID-2000. We generate the center of mass momentum of the np pair ($\vec{p}_{CM} = \vec{p}_1 + \vec{p}_2$) using two models, the distribution of two uncorrelated single nucleons using the ${}^{12}\text{C}$ Argonne V18 momentum distribution for each nucleon and the distribution of a correlated pair using a gaussian distribution in each cartesian direction with $\sigma_x = \sigma_y = \sigma_z = 0.14$ GeV/c (as measured in Refs. [18, 19] and calculated in Ref. [20]). We then calculate the π^+d absorption cross section using the SAID-1998 [21] parametrization. The final momenta of the two protons are generated randomly in phase space from the decay of the $np\pi^+ \rightarrow pp$ system.

Kinematically, it is not possible to distinguish between π^+ absorption on an SRC pair (a pair of nucleons with “small” center-of-mass momentum and “large” relative momentum) and π^+ absorption on an uncorrelated nucleon pair (which happens to be close to each other) because this model is insensitive to the NN relative momentum. In addition, there was almost no difference in the distribution of the two outgoing protons whether we described the center of mass momentum of the np pair absorbing the pion as the sum of two single-nucleon momentum distribution or as the measured correlated pair distribution.

Because the MiniBooNE incident neutrino energies are relatively low (peaked at 0.5 GeV with a tail extending to 2 GeV), the reaction process is dominated by $\Delta(1232)$ production (see Fig. 2). The pion-“deuteron” absorption cross section also peaks at the Δ , further emphasizing the

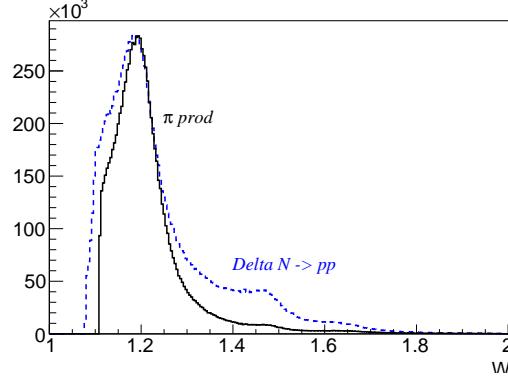


FIG. 2: The invariant mass of the initial proton plus vector boson (e.g., the virtual photon). Black solid line: π production and reabsorption model; blue dashed line: $\Delta N \rightarrow pp$ model.

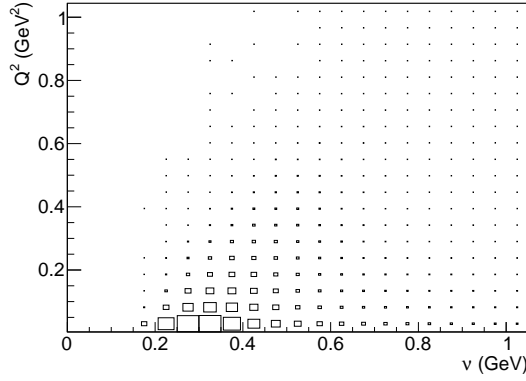


FIG. 3: The momentum transfer squared, Q^2 , plotted versus the energy transfer ν .

Δ peak. The momentum and energy transfer are small, with Q^2 starting at zero and the energy transfer starting at the pion production threshold (see Fig. 3). Because the momentum transfer is small, the momentum of the exchanged pion is also relatively small, peaking at 0.2 GeV/c (see Fig. 4).

The resulting opening angle and momentum distributions of the two protons can be seen in Figs. 5 and 7. The opening angle is predominantly back-to-back and the proton momentum distributions are peaked at about 0.5 GeV/c. These distributions are almost identical for both the two-single-particle and the SRC \vec{p}_{CM} distributions. The transverse missing momentum of the measured particles ($\vec{p}_{miss}^T = \vec{p}_\mu^T + \vec{p}_{p1}^T + \vec{p}_{p2}^T$) is peaked at about 0.2 GeV/c with a long tail extending out to higher momenta (see Fig. 6). The opening angle and momentum distributions of the two protons are consistent with the four observed hammer events. The missing transverse momentum distribution is slightly smaller than the observed $p_{miss}^T \geq 0.3$ GeV/c.

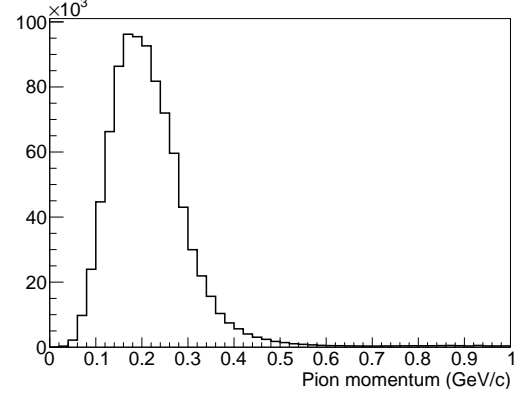


FIG. 4: The momentum of the pion exchanged between the struck nucleon and the np pair.

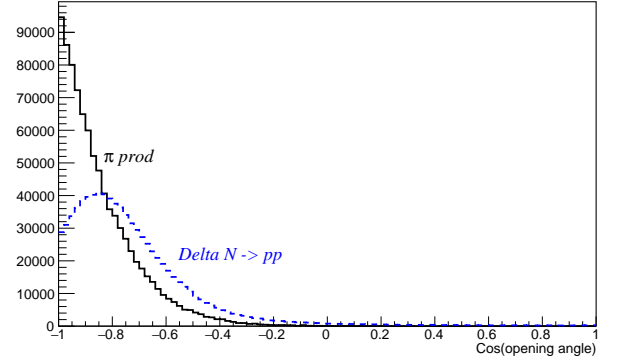


FIG. 5: The cosine of the opening angle of the two final state protons in the lab system. The black solid histogram corresponds to the pion production and reabsorption model and the blue dashed histogram corresponds to the $\Delta N \rightarrow pp$ model. The opening angle distribution was almost identical for the two different center of mass momentum distributions of the NN pair absorbing the π .

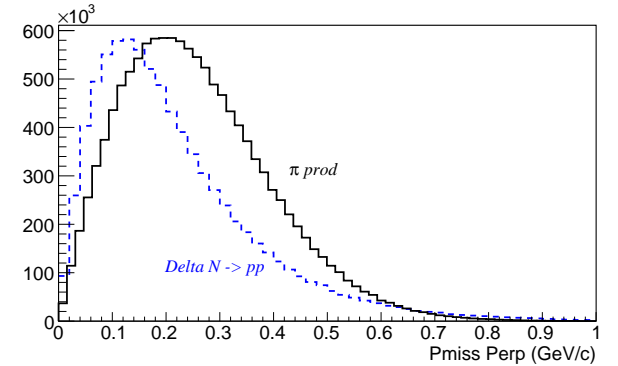


FIG. 6: The perpendicular missing momentum of the muon plus two final state protons in the lab system. The black solid histogram corresponds to the pion production and reabsorption model and the blue dashed histogram corresponds to the $\Delta N \rightarrow pp$ model.

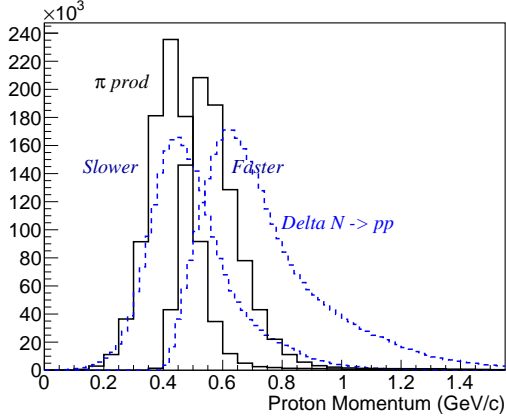


FIG. 7: (color online) The momentum of the two protons in the lab frame, sorted into the slower proton and faster proton. The histograms peaked at $p_p \approx 0.4$ GeV/c correspond to the slower proton and the histograms peaked at $p_p > 0.5$ to 0.6 GeV/c correspond to the faster proton in the event. The solid black large-bin histogram corresponds to the pion production and reabsorption model and the dashed blue small-bin histogram corresponds to the $\Delta N \rightarrow pp$ model.

We also calculated the expected spectra for an incident neutrino energy of 4 GeV, comparable to the average energy of the ArgoNeut neutrino beam. The primary differences in the spectra are that the reaction at these higher neutrino energies covers a much larger range of energy and momentum transfer and a significantly wider range in W . However, the proton spectra are remarkably similar. The two protons are predominantly back-to-back, with momenta peaked at about 500 MeV/c and the same p_{miss}^T distribution.

We also compared these distributions to those from the second reaction model, where the incident neutrino scatters from a nucleon, exciting it to a resonance (N^* or Δ), which then deexcites by colliding with a second nucleon, e.g., $\Delta N \rightarrow pp$. This model generates a nucleon with initial momentum according to the ^{12}C Argonne V18 momentum distribution [16]. It generates the initial electron energy by randomly sampling from the MiniBoone neutrino energy distribution [17]. It then generates the scattered electron energy and angles. It assumes that the inclusive Δ production cross section has the same invariant mass (W) dependence as the $eN \rightarrow e\pi N$ cross section averaged over all outgoing pion momenta. It then generates a second nucleon randomly, and calculates the two-nucleon $\Delta N \rightarrow pp$ distribution randomly by phase space.

The invariant mass distribution in this model is still peaked at the $\Delta(1232)$ mass, although less strongly peaked than the pion production and reabsorption model (Fig. 2). The protons from this model are significantly less back-to-back (Fig. 5), have higher momentum (Fig. 7), and have less missing transverse momentum (Fig. 6)

than the pion production and reabsorption model and appear to agree less well with the four observed hammer events.

There are four possible reaction channels in the pion production and reabsorption model leading to two back-to-back protons in the final state, three for neutrinos and one for anti-neutrinos:

$$\nu \rightarrow \mu^- W^+; \quad W^+ n \rightarrow \pi^0 \mathbf{p}; \quad \pi^0 pp \rightarrow \mathbf{pp} \quad (1)$$

$$\nu \rightarrow \mu^- W^+; \quad W^+ n \rightarrow \pi^+ \mathbf{n}; \quad \pi^+ np \rightarrow \mathbf{pp} \quad (2)$$

$$\nu \rightarrow \mu^- W^+; \quad W^+ p \rightarrow \pi^+ \mathbf{p}; \quad \pi^+ np \rightarrow \mathbf{pp} \quad (3)$$

$$\bar{\nu} \rightarrow \mu^+ W^-; \quad W^- p \rightarrow \pi^0 \mathbf{n}; \quad \pi^0 pp \rightarrow \mathbf{pp} \quad (4)$$

where the nucleons in boldface type are in the final state and can be detected. There is only one reaction channel each for ν and $\bar{\nu}$ that lead to two back-to-back protons plus a neutron in the final state. There are two more ν reaction channels that lead to two back-to-back protons plus a third proton in the final state. There is one reaction channel for the $\Delta N \rightarrow pp$ reaction,

$$\nu \rightarrow \mu^- W^+; \quad W^+ N \rightarrow \Delta; \quad \Delta N \rightarrow \mathbf{pp} \quad .$$

We expect that π absorption on an isospin $T = 1$ NN pair (e.g., pp) will be suppressed by a factor of ten relative to π absorption on a $T = 0$ NN pair. Therefore reaction (1) will be suppressed by a factor of ten relative to reaction (3) which leads to the same final state. We expect that reaction (2), which produces the characteristic hammer signature, will be the same size as reaction (3), which produces the hammer signature plus another proton. Therefore, in this model, there should be equal numbers of hammer events with an extra neutron as with an extra proton. Reaction channel (4) should be ten times smaller than reaction channel (3) so that there should be ten times fewer anti-neutrino events as neutrino events. However, measuring this requires measuring the charge of the outgoing μ .

Because these hammer events appear to be due to a single reaction mechanism, we can use them to determine the incident neutrino energy of the reaction. The reconstructed incident neutrino energy, E_{rec} , depends on the energy, E' , and angle, θ of the outgoing lepton and on the invariant mass of the struck nucleon plus transferred vector boson, $m'^2 = (p_N^\mu + p_B^\mu)^2$ (where p_N^μ and p_B^μ are the four vectors of the struck nucleon and the transferred vector boson respectively):

$$E_{rec} = \frac{m'^2 - m_N^2 + 2m_N E'}{2(m_N - E'(1 - \cos \theta))} \quad (5)$$

We can model the unknown invariant mass of the struck nucleon in several ways (see Fig. 8):

- (“QE”) assume that the neutrino scattered quasielastically from a nucleon ($m' = m_N$);

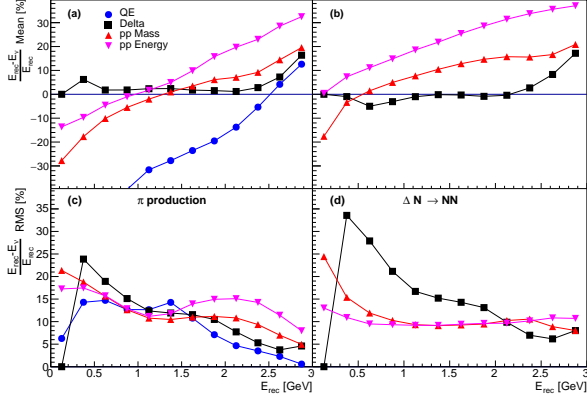


FIG. 8: The fractional error (top) and standard deviation (bottom) of the distribution of the reconstructed beam energy $(E_{rec} - E_\nu)/E_{rec}$ vs the reconstructed beam energy for four ways to calculate the invariant mass of the struck nucleon as described in the text. (left) for the π production and reabsorption model calculated and (right) for the $N\Delta \rightarrow pp$ model. The labels QE, Delta, pp Mass, and pp Energy refer to the four models of the invariant mass of the struck nucleon described in the text.

- (“Delta”) assume that the neutrino scattered from a nucleon, exciting it to a Δ ($m' = m_\Delta = 1.232$ GeV/c²);
- (“pp Mass”) assume that the extra invariant mass of the two protons equals the excitation energy of the struck nucleon ($m' = m_N + (m_{pp} - 2m_N)$); and
- (“pp Energy”) assume that the kinetic energy of the two protons equals the excitation energy of the struck nucleon ($m' = m_N + T_{p1} + T_{p2}$).

Fig. 8 shows the accuracy (mean) and precision (σ) of the reconstructed neutrino energies for both the π production and reabsorption model and the $\Delta N \rightarrow pp$ model. The accuracy is defined as the mean of the $(E_{rec} - E_\nu)/E_{rec}$ distribution and the precision is defined as the RMS of the $(E_{rec} - E_\nu)/E_{rec}$ distribution. In the pion production and reabsorption model, assuming that the struck nucleon is excited to a Δ gives the most accurate reconstruction of the incident neutrino energy over the entire range of energies. Using the two-proton kinetic energy or invariant mass to estimate the excitation energy of the struck nucleon is less accurate. Assuming that the reaction was quasielastic fails completely. In the $\Delta N \rightarrow pp$ model, assuming the struck nucleon is excited to a Δ also gives the most accurate reconstruction of the incident neutrino energy over the entire range of energies.

Assuming that the struck nucleon is excited to a Δ lets us reconstruct the initial neutrino energy to about 30% at 0.5 GeV, improving to $\approx 15\%$ at higher energies.

Summary: The ArgoNeut liquid Argon Time Projection Chamber observed four charged-current neutrino-

argon scattering events with two protons back-to-back in the final state (hammer events). We modeled these hammer events with a simple model where the lepton scatters from a moving nucleon, causing it to emit a π . The π is then absorbed by two nucleons (NN). This pion production and reabsorption process results in events with two back-to-back protons each with momentum of about 500 MeV/c and moderate transverse missing momentum, very similar to that of the observed ArgoNeut events. The results of this model are completely insensitive to the relative momentum of the NN pair and to the choice of its center of mass momentum distribution. This model predicts that a third nucleon is emitted from the nucleus and that about half the time this third nucleon is an easily detectable proton. In this model, the incident neutrino energy can be reconstructed relatively accurately using just the outgoing lepton momentum and angle (for the relatively low MicroBooNE neutrino energies).

We also modeled nucleon excitation, followed by deexcitation via $\Delta p \rightarrow pp$. This process results in two protons that are less similar to the observed events. We should be able to decisively distinguish between the two models by the fraction of hammer events with a third proton.

ArgoNeut hammer events can be described by a simple pion production and reabsorption model. These events can be used to determine the incident neutrino energy, but cannot teach us anything significant about short range correlated NN pairs.

Since the incident neutrino energy of these hammer events can be accurately reconstructed from just the scattered lepton, we suggest that this reaction channel could be used for neutrino oscillation experiments to complement other channels with higher statistics but greater uncertainty in the incident neutrino energy.

We thank O. Palamara, F. Cavanna, and Sam Zeller for many fruitful discussions. This work was partially supported by the US Department of Energy under grants DE-FG02-97ER-41014, DE-FG02-96ER-40960, DE-FG02-01ER-41172 and by the Israel Science Foundation.

* Contact Author weinstein@odu.edu

- [1] U. Mosel, Adv. Nucl. Part. Sci. **66** (2016), 1602.00696.
- [2] K. Egiyan et al. (CLAS Collaboration), Phys. Rev. C **68**, 014313 (2003).
- [3] K. Egiyan et al. (CLAS Collaboration), Phys. Rev. Lett. **96**, 082501 (2006).
- [4] L. Frankfurt, M. Strikman, D. Day, and M. Sargsyan, Phys. Rev. C **48**, 2451 (1993).
- [5] N. Fomin et al., Phys. Rev. Lett. **108**, 092502 (2012).
- [6] E. Piasetzky, M. Sargsian, L. Frankfurt, M. Strikman, and J. W. Watson, Phys. Rev. Lett. **97**, 162504 (2006).
- [7] R. Subedi et al., Science **320**, 1476 (2008).
- [8] I. Korover, N. Muangma, O. Hen, et al., Phys.Rev.Lett. **113**, 022501 (2014), 1401.6138.

- [9] O. Hen et al. (CLAS Collaboration), *Science* **346**, 614 (2014).
- [10] L. Fields et al. (MINERvA Collaboration), *Phys. Rev. Lett.* **111**, 022501 (2013), URL <http://link.aps.org/doi/10.1103/PhysRevLett.111.022501>.
- [11] G. A. Fiorentini et al. (MINERvA Collaboration), *Phys. Rev. Lett.* **111**, 022502 (2013).
- [12] R. Niyazov et al. (CLAS Collaboration), *Phys. Rev. Lett.* **92**, 052303 (2004).
- [13] H. Baghdasaryan et al. (CLAS Collaboration), *Phys. Rev. Lett.* **105**, 222501 (2010), 1008.3100, URL <http://link.aps.org/doi/10.1103/PhysRevLett.105.222501>.
- [14] R. Acciarri et al., *Phys. Rev. D* **90**, 012008 (2014), URL <http://link.aps.org/doi/10.1103/PhysRevD.90.012008>.
- [15] D. Drechsel, O. Hanstein, S. Kamalov, and L. Tia-tor, *Nuclear Physics A* **645**, 145 (1999), ISSN 0375-9474, URL <http://www.sciencedirect.com/science/article/pii/S0375947498005727>.
- [16] R. B. Wiringa, R. Schiavilla, S. C. Pieper, and J. Carlson, *Phys. Rev. C* **89**, 024305 (2014).
- [17] A. A. Aguilar-Arevalo et al. (MiniBooNE Collaboration), *Phys. Rev. D* **79**, 072002 (2009), URL <http://link.aps.org/doi/10.1103/PhysRevD.79.072002>.
- [18] A. Tang et al., *Phys. Rev. Lett.* **90**, 042301 (2003).
- [19] R. Shneor et al., *Phys. Rev. Lett.* **99**, 072501 (2007).
- [20] C. Ciofi degli Atti and S. Simula, *Phys. Rev. C* **53**, 1689 (1996), URL <http://link.aps.org/doi/10.1103/PhysRevC.53.1689>.
- [21] C. H. Oh, R. A. Arndt, I. I. Strakovsky, and R. L. Workman, *Phys. Rev. C* **56**, 635 (1997), URL <http://link.aps.org/doi/10.1103/PhysRevC.56.635>.